

See discussions, stats, and author profiles for this publication at: <https://www.researchgate.net/publication/263740354>

Characterization of Naphthenic Acids by Gas Chromatography–Fourier Transform Ion Cyclotron Resonance Mass Spectrometry

ARTICLE in ANALYTICAL CHEMISTRY · JULY 2014

Impact Factor: 5.64 · DOI: 10.1021/ac501549p · Source: PubMed

CITATIONS

4

READS

49

9 AUTHORS, INCLUDING:



Kerry Peru

Environment Canada

116 PUBLICATIONS 1,997 CITATIONS

[SEE PROFILE](#)



Dena W McMartin

University of Regina

64 PUBLICATIONS 694 CITATIONS

[SEE PROFILE](#)



John Headley

Environment Canada

219 PUBLICATIONS 3,298 CITATIONS

[SEE PROFILE](#)

Characterization of Naphthenic Acids by Gas Chromatography-Fourier Transform Ion Cyclotron Resonance Mass Spectrometry

Xavier Ortiz,^{†,‡} Karl J. Jobst,[†] Eric J. Reiner,[†] Sean M. Backus,[‡] Kerry M. Peru,[§] Dena W. McMartin,^{||} Gwen O'Sullivan,[⊥] Vince Y. Taguchi,^{*,†} and John V. Headley[§]

[†]Ontario Ministry of the Environment and Climate Change, 125 Resources Road, Toronto, Ontario M9P 3V6, Canada

[‡]Canada Centre for Inland Waters, Environment Canada, 867 Lakeshore Road, Burlington, Ontario L7R 4A6, Canada

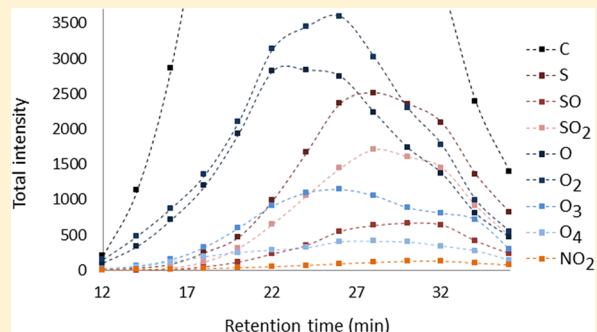
[§]Aquatic Contaminants Research Division, Water Science and Technology Directorate, Environment Canada, 11 Innovation Boulevard, Saskatoon, Saskatchewan S7N 3H5, Canada

^{||}Environmental Systems Engineering, University of Regina, 3737 Wascana Parkway, Regina, Saskatchewan S4S 0A2, Canada

[⊥]Department of Environmental Science, Mount Royal University, 4825 Mount Royal Gate, Calgary, Alberta T3E 6K6, Canada

Supporting Information

ABSTRACT: During the bitumen extraction from the oil sands of Alberta, large volumes of process water containing naphthenic acids are stored in tailing ponds. The naphthenic acids along with other components in the processed waters are known to be toxic in aquatic environments. In view of the complex matrix and the toxicity of the processed waters, there is a need for complementary analytical techniques for comprehensive characterization of the naphthenic acid mixtures. This study reports the online gas chromatographic separation of naphthenic acid mixtures prior to ultrahigh resolution mass spectrometry detection, using electron and chemical ionization. Two oil sands processed water samples and two groundwater samples were characterized to evaluate the performance of the instrumental technique. The high mass resolution of the system enabled visualization of the data using Kendrick mass defect plots. The addition of gas chromatographic separations enabled visualization of the data as unique compound class elution fingerprints. The technique is demonstrated to be a valuable tool for chemical fingerprinting of naphthenic acids.



Bitumen extracted from the oil sands of Alberta (Canada) constitute one of the world's largest fuel reserves, producing 705 million barrels during 2012 with an ultimate potential of 315 billion barrels.¹ Oil is recovered from the bitumen using an alkaline hot water extraction process, which requires approximately three barrels of water for every barrel of crude oil. Due to the zero discharge policy for oil sands process water (OSPW), these extracts are stored in large tailing ponds, consisting of a slurry of sand, silt, clay and a residual fraction of the bitumen containing naphthenic acids.^{2,3}

Naphthenic acids (NAAs) are carboxylic acids containing at least one saturated ring in their structure, although this term is now commonly used to describe the wide range of organic acids found in crude oil, which can be up to a 4% w/w.⁴ Classical structures are represented by the general chemical formula $C_nH_{2n+z}O_2$, where n is the carbon number and z the hydrogen deficiency and is a negative, even integer.⁵ The molecular weights differ by 14 Da (CH_2) between n -series and two Da (H_2) between z -series. However, the acid fraction of oil sands processed water is now known to also include a wide range of heteroatomic species, containing S, N and O aromatic components. Thus, the naphthenic acid fraction compounds (NAFCs) of oil sands samples are often classified according to

the heteroatoms present in their structures (e.g., a compound containing an atom of sulfur and three atoms of oxygen would belong to the SO_3 compound class, regardless of the carbon number and hydrogen deficiency). Due to the complexity of NAFCs, a large number of isomers will exist for a given n and z homologue or compound class, although in most structures, the carboxylic acid group is usually attached to the aliphatic chain rather than the saturated ring.^{6–8}

Interest in the characterization of NAAs (and NAFCs) has increased steadily in recent years due in part to new initiatives such as the joint Alberta-Canada oil sands monitoring program. Studies have measured the toxicity of NAFCs in rats, fish, birds, plankton and wetland plants.^{9–11} Concentrations of NAAs in oil sands processed waters range from 40 to 130 mg L⁻¹, whereas concentration in the Athabasca River and nearby lakes is usually below 1 mg L⁻¹.^{12,13} Naphthenic acid fraction compounds are also implicated in the corrosion of pipelines and other structures used to transport and store the oil.^{14,15}

Received: April 28, 2014

Accepted: July 6, 2014

Published: July 6, 2014



In the past, gas chromatography coupled to Fourier transform infrared spectroscopy (GC-FTIR) has been used for the analysis of derivatized NAs.^{13,16} However, the GC-FTIR technique can overestimate concentrations of NAs, in part due to its inability to resolve the presence of other organic acids in the mixture. Naphthenic acids fraction compounds are usually eluted as an unresolved trace in the GC.^{13,16} Significantly improved chromatographic resolution can be attained with comprehensive two-dimensional GC coupled to time-of-flight mass spectrometry (GCxGC-TOFMS). This technique has led to the recent characterization of individual NAs, but complete chromatographic separation of the NAFC mixture has not been achieved.^{17–20} High-performance liquid chromatography tandem MS (HPLC-MS/MS) applications to date have focused primarily on quantitative analysis of classical NAs structures, using targeted characterization of the sample.²¹ Liquid chromatography-time-of-flight mass spectrometry (LC-TOFMS) and other medium mass resolution detection methods of NAFC have been reported in the literature.²² Some low and medium resolution methods may not distinguish among compound classes (e.g., to resolve the ions $C_{19}H_{29}S^+$ and $C_{22}H_{25}^+$, a resolving power of 80 000 full width at half-maximum, fwhm, is needed).^{22,23} Consequently, for optimum resolving power and characterization of oil sands NAFCs, it is desirable to couple (gas or liquid) chromatographic separation to (ultra)high resolution MS.

Due to its unique resolving power (theoretically over 1 000 000), FTICR MS is the preferred technique for NAFC characterization.^{24,25} Naphthenic acid fraction compound samples are generally injected by direct infusion with electrospray ionization (ESI),²⁶ atmospheric pressure chemical ionization (APCI)²⁷ or atmospheric pressure photoionization (APPI),²⁸ to provide complementary characterization of a given sample.²⁹ Nevertheless, direct infusion of the samples limits the ability to distinguish structural isomers. The benefit of chromatographic separation was demonstrated in a recent study in which NAFC mixtures were prefractionated with offline (ultrahigh performance) LC prior to FTICR MS analysis, leading to the detection of twice the number of components identified using direct infusion.²⁹

In view of the improved coverage prefractionation or chromatographic separation offers for comprehensive characterization of complex mixtures, the present study reports the online gas chromatographic separation of NAFC mixtures prior to ultrahigh resolution mass spectrometry detection (GC-FTICR MS). This study also compares the behavior of NAFCs under different ionization conditions, including electron ionization (EI) and chemical ionization with methane ($Cl-CH_4$) and ammonia ($Cl-NH_3$), in order to complement the previously published FTICR MS ionization techniques for naphthenic acids.^{26–28} The goal is to gain a wider coverage of components present in the oil sands samples for environmental forensics. The GC-FTICR MS technique was evaluated based on the characterization of four NAFC extracts from different origins. It will be shown that GC-FTICR MS offers unique visualization of the results that illustrate the chromatographic separation of the different NAFC classes as compound class elution fingerprints.

EXPERIMENTAL SECTION

Samples. To evaluate the performance of GC-FTICR MS for the characterization of NAFC mixtures, two oil sands processed water samples (OSPW1 and OSPW2) and two

groundwater samples (GW1 and GW2) from the Athabasca River region were investigated. Oil sands process water samples were collected during June of 2011, in 4 L solvent rinsed amber glass bottles. Groundwater samples were collected likewise between May and July of 2011. Samples were filtered under vacuum, acidified to $pH = 4.5$ and extracted using Strata X-A solid phase extraction sorbent (Phenomenex, Torrance, CA).³⁰ For GC analysis of NAFCs, the extracts were methylated using BF_3 /methanol.³¹

Instrumentation. Derivatized NAFC mixtures were analyzed with a Varian GC-TQ(triple quadrupole)-FTICR MS (Varian Inc., Walnut Creek, CA), consisting of a Varian CP-8400 autosampler, a Varian 3800 GC, a Varian 920 TQ-FTICR MS and a Varian 9.4 T superconducting magnet.^{32,33} The GC was fitted with a DB5-MS capillary column (40 m, 0.18 mm i.d., 0.18 μ m film thickness) from Agilent (Santa Clara, CA). Samples were injected (1 μ L) in splitless mode at 230 °C. The carrier gas was helium at 0.5 mL min⁻¹ constant flow mode. The oven was set at 40 °C for 1 min, increased at 30 °C min⁻¹ to 160 °C, increased at 5 °C min⁻¹ to 300 °C and held for 10 min. The TQ was operated in the EI mode (70 eV) and the CI mode with methane and ammonia (70 eV, 3.0 Torr) and was set to pass all ions. The FTICR MS was operated at a resolving power of 100 000 to 150 000 (fwhm). Mass spectra were obtained using arbitrary waveform excitation and broadband detection from m/z 75 to 650. Detection and cycle times were set at 524 ms and 1.5 s, respectively. External mass calibration was performed using perfluorotributylamine (PFTBA), and internal mass calibration was performed using protonated diisonyl phthalate (background ion) at m/z 419.315 60.

QA/QC. Samples were run in triplicate with solvent blanks run between experimental runs to ensure no carryover between samples. The mass spectrometer was mass calibrated using conventional standards. Specifically, external mass calibration was performed using perfluorotributylamine (PFTBA), whereas each mass spectrum was internally calibrated using a background phthalate ion (protonated diisonyl phthalate) at m/z 419.315 60. The performance of the GC was optimized based on previous reports of GC of OSPW with Orbitrap MS detection of the methyl esters.³⁰ The volatile esters are reproducibly transferred to the GC quantitatively with greater than 80% efficiency/recovery. The GC time could be made longer or shorter but the gains are minimal as the NAFC elute as a complex unresolved chromatogram as previously reported in the literature for one-dimensional GC analyses of OSPW.²³

Kendrick Mass Defect Plots. By convention, the International Union of Pure and Applied Chemistry (IUPAC) has defined a mass scale based on the carbon exact mass ($C = 12.000\ 00$ Da). Kendrick realized that by using a mass scale based on CH_2 (i.e., the Kendrick mass scale, where $CH_2 = 14.000\ 00$ Da), homologous series of hydrocarbons can be readily identified because of their common mass defect (difference between exact mass and nominal mass).³⁴ The conversion is performed by multiplying the IUPAC mass by 14.000 00 and dividing by 14.015 65. For example, Kendrick exact masses for methane (16.013 40 Da), ethane (30.013 40 Da) and propane (44.013 40 Da) share the same mass defect (0.013 40 Da) regardless of the different elemental compositions. Accordingly, each series of hydrocarbons containing different heteroatoms in their structures (commonly O, S or N) or a different number of double bonds will have unique mass defects. This feature is the basis for the Kendrick mass defect

plot, where Kendrick mass defect (*y*-axis) is plotted against Kendrick exact mass (*x*-axis). Complex FTICR mass spectra containing thousands of peaks are thus visualized in a simplified plot where each hydrocarbon series (belonging to a different compound class or having a different hydrogen deficiency) is aligned horizontally.^{33,35} Kendrick mass defect plots were used in the present study to identify the different NAFC compound classes. Elemental compositions were assigned according to the exact mass and hydrocarbon series belonging to a particular compound class were identified by the difference(s) of 14.000 00 Kendrick mass units ($\pm\text{CH}_2$) or 1.0067 Kendrick mass units (\pm hydrogen deficiency). Kendrick mass defect plots were constructed using Microsoft Excel. Elemental composition assignments were performed using a combination of custom macros for Excel as well as Elemental Composition Calculator (Varian Inc.). For the calculations, 0–100 of the elements C, H, N, O and S were considered. For all assignments, the accurate mass measurements were within 5 ppm of the theoretical value.

RESULTS AND DISCUSSION

Compound Class Assignment. Due to the ultrahigh resolution of FTICR MS, each mass spectrum can show up to several thousand peaks, as is the case with the spectrum (Figure 1a) obtained from OSPW2. It is acknowledged that visualization of the extremely large data sets is still a work in progress. There is no clear visualization method that provides information on ion classes, relative abundances and molecular weight distribution all on the same plot for such large data sets. For this reason, as described in the Experimental Section, Kendrick mass defect plots were used as a visual aid for the assignment of elemental compositions. Figure 1b displays the Kendrick mass defect plot obtained from the mass spectrum of Figure 1a. The FTICR MS, although theoretically capable of a resolving power of 1 000 000, was operated at 100 000 to 150 000 fwhm due to the cycle time constraints imposed by the GC. Nevertheless, most of the possible NAFC compound classes could be distinguished. Common compound classes in the oil sands process water and groundwater samples were C, S, SO, SO₂, O, O₂, O₃, O₄, N, NO, NO₂ and NO₃, although the relative abundances depended on the ionization technique, which will be discussed below. The C class here represents ions without heteroatoms and therefore covers the wide range of hydrocarbons that are prevalent in petroleum mixtures. The C class also includes hydrocarbon fragments derived from heteroatom containing ions. The O₂ class is expected to be composed of derivatized naphthenic acids. However, other O₂ compounds (e.g., polyalcohols, ethers, ketones, esters) and fragment ion structures cannot be ruled out without significantly improved chromatography and deconvolution algorithms that are not yet available. There were only a few cases where compound class assignments were, at first glance, somewhat ambiguous. For example, to distinguish C₁₄H₂₆SO₄⁺ (*m/z* = 290.1546) and C₂₀H₂₀NO⁺ (290.1539), a mass resolving power of 400 000 would be needed. In this case, the mass difference corresponds to 2.5 ppm, whereas the accuracy of FTICR mass measurements can be within 1 ppm.^{36,37} Indeed, the Kendrick mass defect plot of the SO₄/NO classes (Figure 1c) displays two distinct clusters of peaks and, based upon mass accuracy alone, it would appear that the lower mass cluster is composed of NO ions, whereas the higher mass cluster is mainly composed of SO₄ ions. In some cases, such as the low *m/z* ions belonging to the NO class, only one compound class is possible according to the degree of

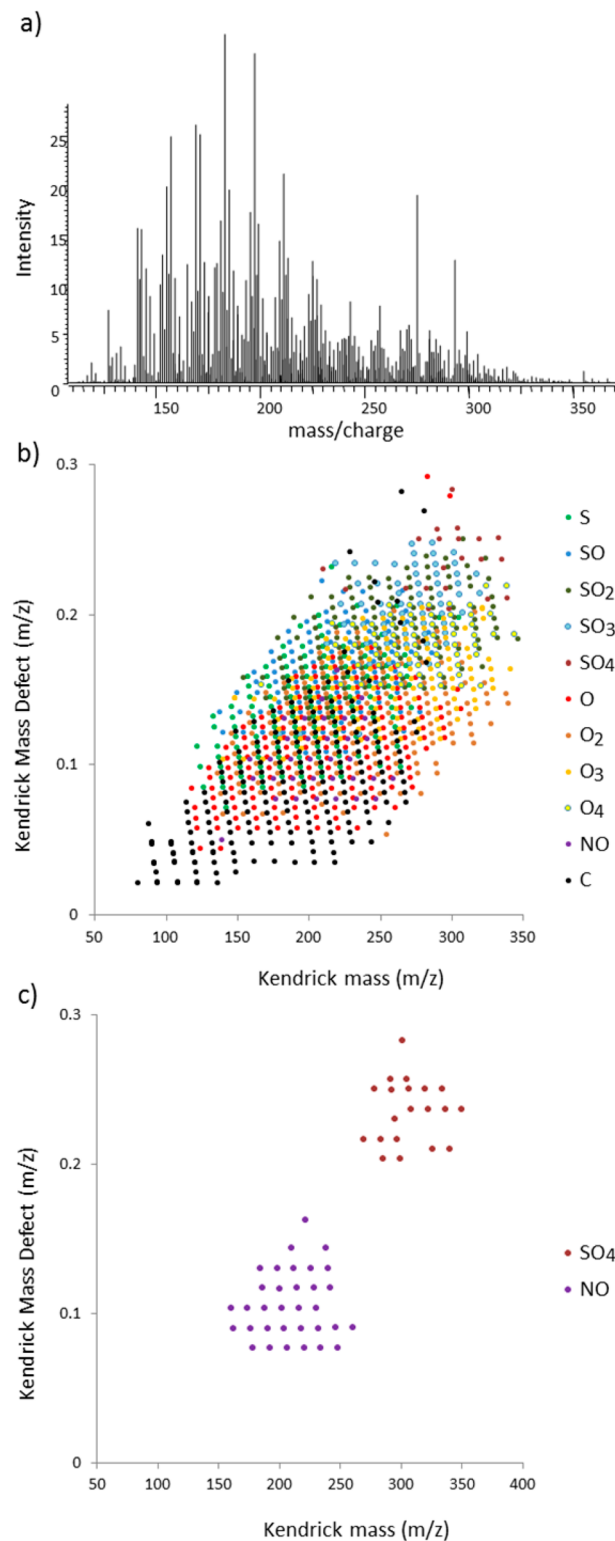


Figure 1. (a) FTICR MS mass spectrum obtained from an oil sands processed water sample (OSPW2) under EI conditions; (b) Kendrick Mass Defect plot of the various compound classes identified in OSPW2; (c) Kendrick Mass Defect plot of NO/SO₄ compound classes for OSPW2 in the EI mode.

unsaturation. Nevertheless, we cannot rule out the possibility that the ions displayed in Figure 1c represent a mixture of SO₄/NO ions that would necessitate increased resolving power. The

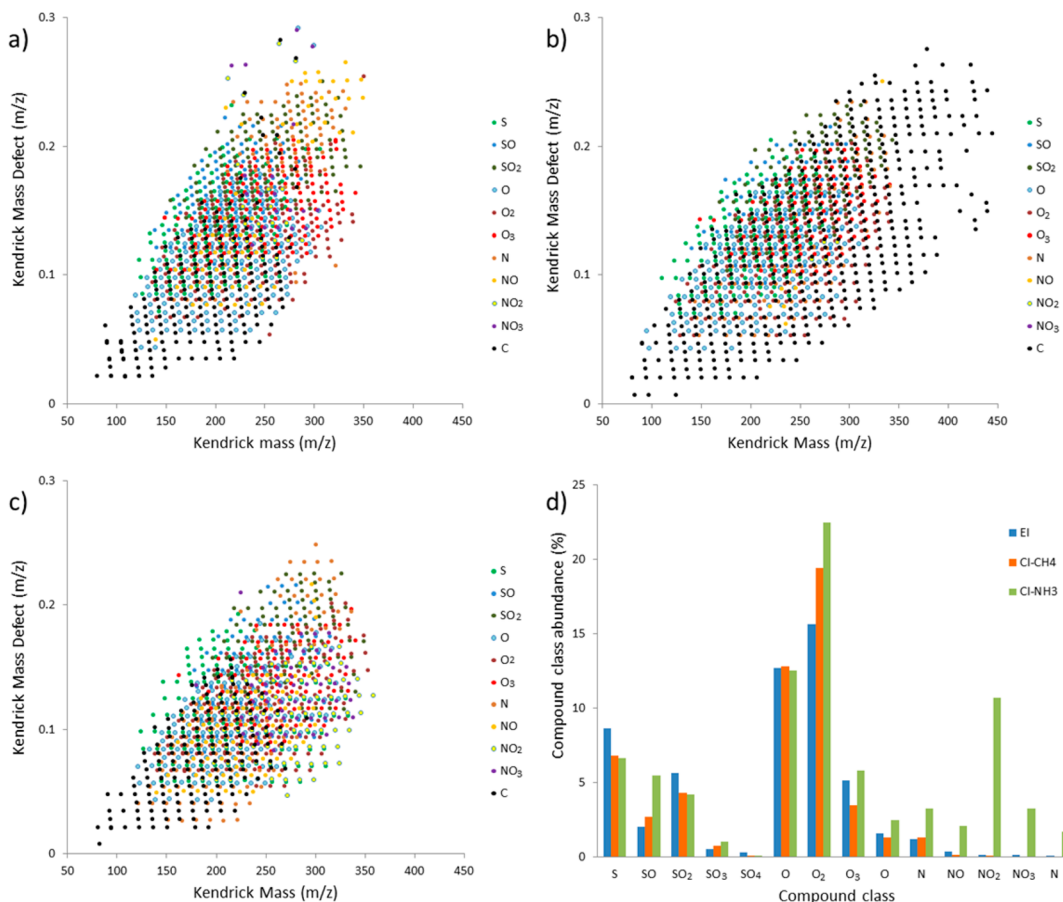


Figure 2. Kendrick plots for OSPW2 using EI (a), CI-CH₄ (b), CI-NH₃ (c) and compound class abundance (d). Precision of the measurements (made in triplicate) was within 15% relative standard deviation (RSD).

same mass behavior was observed for the SO₃/N ions observed under CI conditions discussed in the next Section.

Ionization of Naphthenic Acids. For the NAFC ionization, three different techniques were compared: EI, CI-CH₄ and CI-NH₃. Figure 2 shows the Kendrick mass defect plots obtained from OSPW2 for each different kind of ionization. The total number of ions detected using the different ionization techniques were similar. For this sample, 2263, 1947 and 2108 peaks were detected using EI, CI-CH₄ and CI-NH₃, respectively. Prima facie, this observation is surprising because EI (Figure 2a) typically results in more fragmentation than CI. Note that although NAFC contain at least two oxygen atoms in their structures, not all ions in the Kendrick mass spectra belonged to O₂ class. In fact, the most abundant class of ions was the C class, which undoubtedly include hydrocarbon ions that result from fragmentation of the NAFCs. Because the NAFCs have been derivatized to the corresponding methyl esters prior to sample analysis, these ions should undergo consecutive losses of CH₃O⁻ and CO under EI conditions. This is indeed the case for a typical NA methyl ester, methylcyclopentane carboxylate,³⁸ which displays a very weak molecular ion and an intense peak corresponding to losses of CH₃O⁻ and CO.

CI-CH₄ (Figure 2b) produced higher mass ions than EI, but still, fragmentation of NAFC could not be avoided. Most of the higher mass ions correspond to the C class, which is likely the result of dissociation. The explanation for this observation may lie in the difference in proton affinities (543 kJ mol⁻¹ for CH₄ and around 850 kJ mol⁻¹ for hydrocarbon methyl esters).³⁷

The dissociation chemistry of protonated methyl esters (RCOOCH₃) is well documented.³⁹ Considering the high internal energy (c. 300 kJ/mol) of the incipient M + H⁺ ions, the abundant C class ions may well result from fragmentation of the M + H⁺ ions by consecutive losses of CH₃OH and CO.³⁹ Another potential mechanism for formation of higher mass ions can be the formation of alkyl adducts [M + R]⁺. It is known that the use of CH₄ as a reagent gas, apart from the methonium ion (CH₅⁺), results in the formation of other reagent ions (e.g., C₂H₅⁺, C₃H₇⁺) that could potentially attach to M.³⁹

When NH₃ was used as the reagent gas, the high mass C ions were not detected, see Figure 2c. This may be because the proton affinity of NH₃ (853 kJ/mol) is slightly higher than that of the higher mass NAs, and thus proton transfer does not take place. Nevertheless, the abundance of N, NO, NO₂, NO₃ and N₂ compound classes were significantly enhanced (Figure 2d). This points to the formation of NH₃ adducts or other ion–molecule reactions.³⁹

The abundance profile of the various compounds classes of OSPW2 (Figure 2d) show some interesting differences, one example being the formation of NH₃ adducts under CI-NH₃ conditions. Overall, CI enhances the abundance of the O₂ class of ions as well as other heteroatom classes.

Chromatographic Separation of Naphthenic Acids. The online GC step prior to the FTICR MS facilitated partial separation of the components eluting from 10 to 40 min as evidenced by the unresolved trace observed for the total ion chromatogram. Although the components are not baseline resolved, the separation over 30 min, as opposed to direct

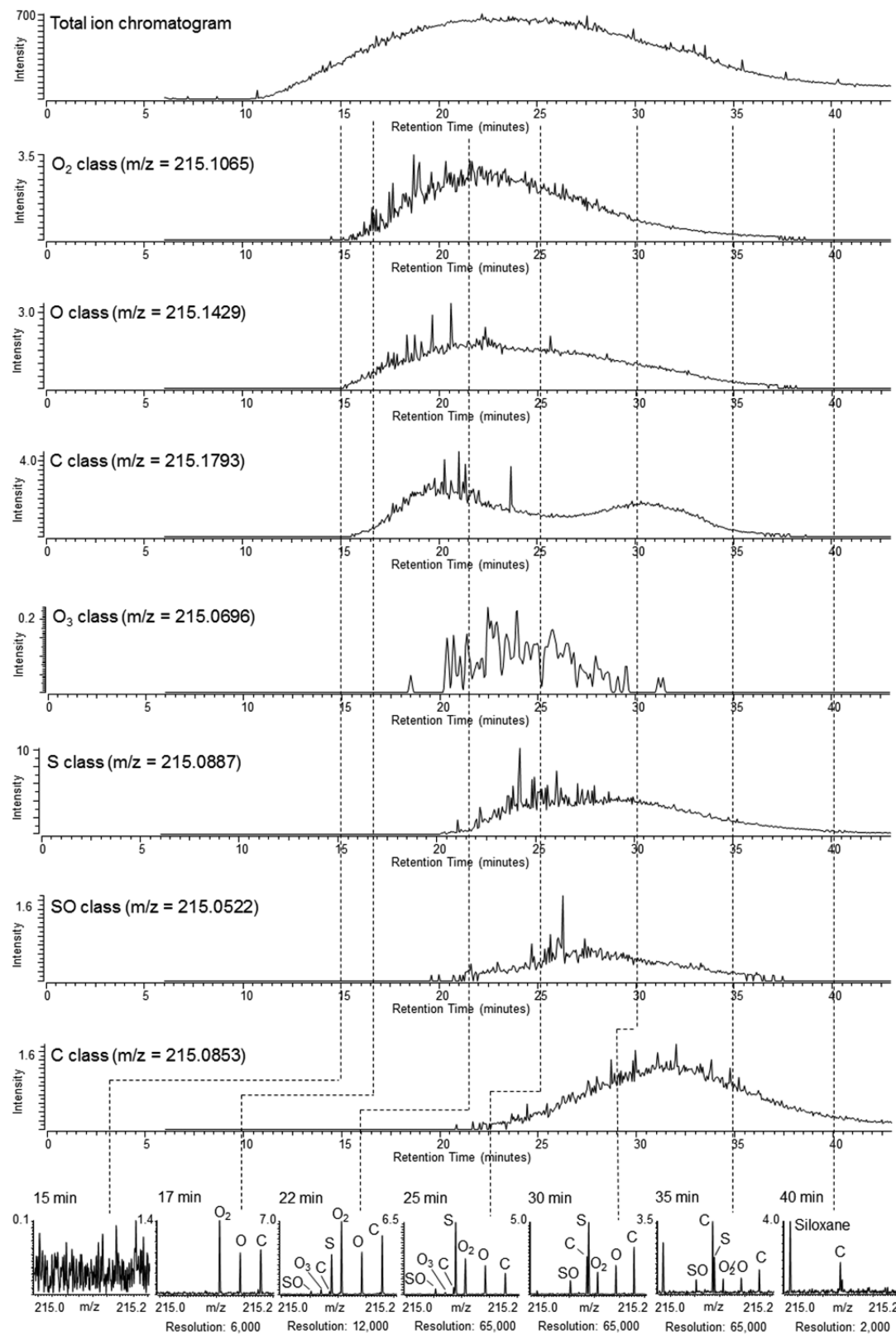


Figure 3. Chromatographic separation of isobaric compounds of OSPW2 at $m/z = 215$.

infusion, facilitated the partial separation of isobaric compound classes. Figure 3 shows an example for the isobaric compounds of OSPW2 at $m/z = 215$. At this nominal mass, seven isobaric ions belonging to six different compound classes were found: $C_{16}H_{23}^+$ ($m/z = 215.1794$, C class), $C_{17}H_{11}^+$ ($m/z = 215.0855$,

C class), $C_{15}H_{19}O^+$ ($m/z = 215.1436$, O class), $C_{14}H_{15}O_2^+$ ($m/z = 215.1067$, O₂ class), $C_{13}H_{11}O_3^+$ ($m/z = 215.0703$, O₃ class), $C_{14}H_{15}S^+$ ($m/z = 215.0889$, S class) and $C_{13}H_{11}SO^+$ ($m/z = 215.0525$, SO class). As shown in Figure 3, each compound class yields a chromatographic apex at different retention times.

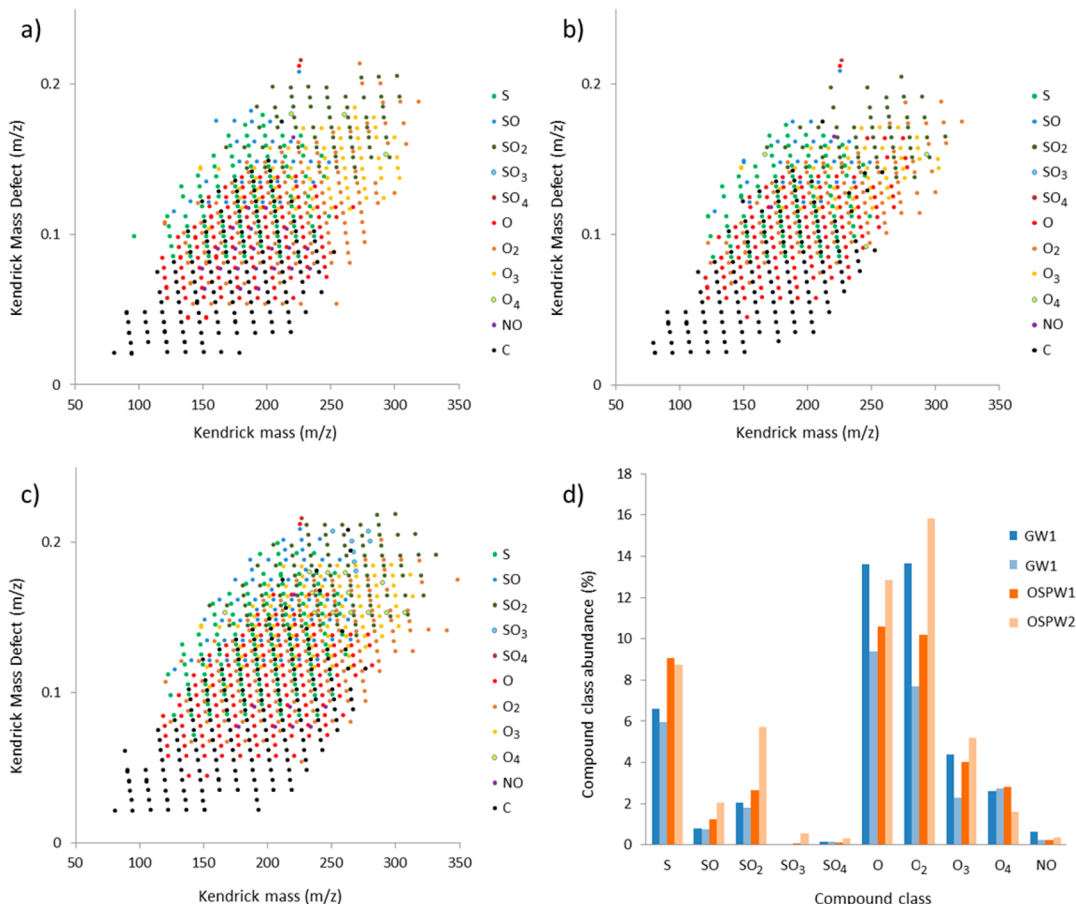


Figure 4. Kendrick mass defect plots of GW1 (a), GW2 (b), OSPW1 (c) and compound class abundance (d), min 10–40. Precision of the measurements (made in triplicate) was within 15% RSD.

Note that in order to distinguish all peaks simultaneously without prior GC separation, a resolution of 65 000 is needed. GC separation enables certain target ions to be monitored using a significantly reduced resolving power. For example, see Figure 3 (bottom) at a retention time of 17 min: C, O and O₂ classes could be distinguished operating at 6000 resolving power. At a retention time of 22 min: C, O, O₂ and S classes were distinguished at 12 000 resolving power.

As shown in Figure 3, the O and O₂ compound classes eluted first, followed by the O₃ class. The SO_x compound classes were generally observed at the longest retention times investigated. Of the two *m/z* 215 ions (C₁₆H₂₃⁺ and C₁₇H₁₁⁺), the more saturated components eluted first. These trends are mirrored by all the other ions detected in the mixture (see the Supporting Information). As expected, fragments with lower *m/z* and mass defect eluted earlier than those with higher *m/z* and mass defect.

The addition of chromatographic separation prior to the FTICR MS analysis facilitates plots of the compound class histograms as a function of retention time. This visualization can be based on either (i) time-resolved specific components that differ by carbon or Z number within a given compound class (see the Supporting Information); or (ii) time-resolved total intensity for all species within a given compound class. This representation of the results reveals unique fingerprints for the samples of this study, see below.

Oil Sands Processed Water and Groundwater Samples.

Figure 4 shows the Kendrick plot for GW1, GW2

and OSPW1 in EI mode (OSPW2 is presented in Figure 1b). Plots were generated by combining the mass spectra for the chromatographic trace (10–40 min). Approximately 1300 (GW1, GW2 and OSPW1) and 2200 peaks (OSPW2) were detected, corresponding to 11 different compound classes.

Figure 4d shows the histogram of the total intensity of each compound class for the whole trace of GW1, GW2, OSPW1 and OSPW2 (min 10–40). Apart from the C class (which was omitted in the figure due to its high intensity), the most abundant compound classes observed were the O₂ class (8–16%), O class (9–14%) and S class (6–9%). This type of visualization is widely used in petroleomics studies²⁴ but, in this particular case, significant differences among samples are not readily apparent.

Figure 5a–d plots intensities of the various compound classes (generated under EI conditions) against the retention time for the OSPW and groundwater samples in this study. The chromatographic trace, shape, intensity and retention time apex were characteristic of each compound class for each sample. These features were also observed for some classes with the same elemental composition and may therefore suggest differing structures of isomeric compounds. Ratios between compound classes were also unique for each NAFC mixture. For example, whereas O and O₂ ratios and peak shapes were similar in GW1 and OSPW1, the O class was more abundant in GW2 whereas the O₂ class was more abundant in OSPW2. Also, O and O₂ classes had a more intense apex than S class in

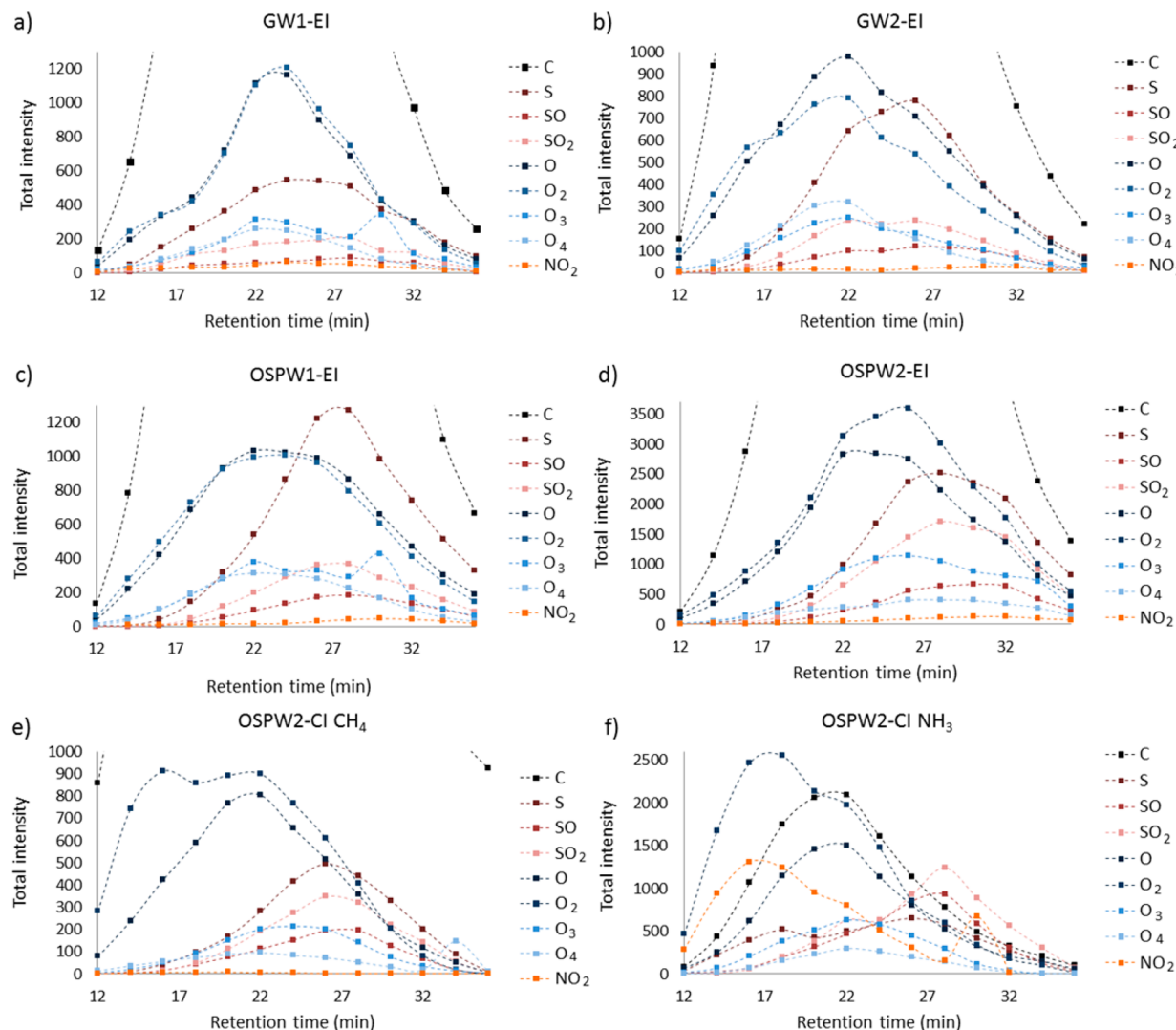


Figure 5. GC separation of NAFC classes of GW1 (a), GW2 (b), OSPW1 (c) and OSPW2 in EI(d), CI-CH₄ (e) and CI-NH₃ (f) mode. C class apex intensities were 4.8 kcounts (GW1-EI), 6.8 kcounts (GW2-EI), 6.0 kcounts (OSPW1-EI), 11.7 kcounts (OSPW2-EI), 3.7 kcounts (OSPW2-CI CH₄) and 2.1 kcounts (OSPW2-CI NH₃).

GW1 and OSPW2, whereas they were similar in GW2 while S class was more intense than O and O₂ class in OSPW1.

Different compound class elution profiles, obtained from fragments as well as molecular ions or protonated molecules, were observed for each sample using EI, CI-CH₄ or CI-NH₃ (Figure 5d–f). EI was the most energetic ionization technique employed in this study, and as a result, the C class was most abundant due to fragmentation of the NAFCs. In contrast, the C class was not very abundant when CI-NH₃ was used (see Figure 5f) but N-containing classes were enhanced. CI-CH₄ ionization offered intermediate results, with a C class apex lower than in EI but higher than in CI-NH₃ and a relative O₂ class abundance higher than in EI but lower than in CI-NH₃.

CONCLUSIONS

In the present study, GC-FTICR MS with EI, CI-CH₄ and CI-NH₃ ionization has been successfully applied to the characterization of four samples with different distributions of NAFCs. The addition of chromatographic separation prior to the ultrahigh resolution MS detection produced unique fingerprints when the intensity of each compound class was plotted against retention time. The distribution and composition of observed

NAFC ions was also influenced by the ionization technique and choice of chemical ionization reagent. GC-FTICR MS is thus complementary to existing atmospheric pressure ionization-based methods for characterizing complex NAFC mixtures. The ability to time resolve isobaric compounds and compound classes in complex NAFC mixtures is expected to enhance the quality of ongoing studies in oil sands environmental forensics.

ASSOCIATED CONTENT

S Supporting Information

Detailed information about the Kendrick plots of eluted NAFCs at different retention times, compound class histograms of eluted NAFCs at different retention times and time-resolved specific components within O₂ compound class. This material is available free of charge via the Internet at <http://pubs.acs.org>.

AUTHOR INFORMATION

Corresponding Author

*Vince Y. Taguchi. E-mail: Vince.Taguchi@ontario.ca. Phone: +1 416 235 5902. Fax: +1 416 235 5744.

Author Contributions

The paper was written through contributions of all authors. All authors have given approval to the final version of the paper.

Notes

The authors declare no competing financial interest.

ACKNOWLEDGMENTS

The authors acknowledge Dr. Jason Ahad for providing the derivatized sample extracts. Dr. Xavier Ortiz acknowledges the Natural Sciences and Engineering Research Council of Canada (NSERC) for the Visiting Fellowship award.

REFERENCES

- (1) Teare, M.; Burrowes, A.; Baturin-Pollock, C.; Rokosh, D.; Evans, C.; Marsh, R. *Alberta's Energy Reserves 2012 and Supply/Demand Outlook 2013–2022*; Report ST98-2012; Energy Resources Conservation Board, Government of Alberta: Calgary, Alberta, 2013. <http://www.aer.ca/data-and-publications/statistical-reports/st98> (accessed January 21, 2014).
- (2) Headley, J. V.; Peru, K. M.; Mishra, S.; Meda, V.; Dalai, A. K.; McMartin, D. W.; Mapolelo, M. M.; Rodgers, R. P.; Marshall, A. G. *Rapid Commun. Mass Spectrom.* **2010**, *24*, 3121–3126.
- (3) Grewer, D. M.; Rozlyn, R. F.; Whittal, R. M.; Fedorak, P. M. *Sci. Total Environ.* **2010**, *23*, 5997–6010.
- (4) Headley, J. V.; Peru, K. M. *Anal. Chem.* **2007**, *79*, 6222–6229.
- (5) Scott, A. C.; MacKinnon, M. D.; Fedorak, P. M. *Environ. Sci. Technol.* **2005**, *39*, 8388–8394.
- (6) Dzidic, I.; Somerville, A. C.; Raia, J. C.; Hart, J. V. *Anal. Chem.* **1988**, *60*, 1318–1323.
- (7) Fan, T. P. *Energy Fuels* **1991**, *5*, 371–375.
- (8) Clemente, J. S.; Prasad, N. G. N.; MacKinnon, M. D.; Fedorak, P. M. *Chemosphere* **2003**, *50*, 1265–1274.
- (9) Rogers, V. V.; Wickstrom, M.; Liber, K.; MacKinnon, M. D. *Toxicol. Sci.* **2002**, *66*, 347–355.
- (10) Zhang, X.; Wiseman, S.; Yu, H.; Liu, H.; Giesy, J. P.; Hecker, M. *Environ. Sci. Technol.* **2011**, *45*, 1984–1991.
- (11) Frank, R. A.; Kavanagh, R.; Burnison, B. K.; Arsenault, G.; Headley, J. V.; Peru, K. M.; Van Der Gaak, G.; Solomon, K. R. *Chemosphere* **2008**, *72*, 1309–1314.
- (12) Yen, T. W.; Marsh, M. D.; MacKinnon, M. D.; Fedorak, P. M. J. *Chromatogr. A* **2004**, *1033* (1), 83–90.
- (13) Holowenko, F. M.; MacKinnon, M. D.; Fedorak, P. M. *Water Res.* **2001**, *35*, 121–134.
- (14) Da Campo, R.; Barrow, M. P.; Sheperd, A. G.; Salisbury, M.; Derrick, P. J. *Energy Fuels* **2009**, *23*, 5544–5549.
- (15) Mohammed, M. A.; Sorbie, K. S. *Colloids Surf., A* **2009**, *349*, 1–18.
- (16) Young, R. F.; Coy, D. L.; Fedorak, P. M. *Anal. Methods* **2010**, *2*, 765–770.
- (17) Rowland, S. J.; West, C. E.; Scarlett, A. G.; Jones, D.; Frank, R. A. *Rapid Commun. Mass Spectrom.* **2011**, *25*, 1198–1204.
- (18) Sheperd, A. G.; Van Mispelaar, V.; Nowlin, J.; Genwit, W.; Grutters, M. *Energy Fuels* **2010**, *24*, 2300–2311.
- (19) Rowland, S. J.; Scarlett, A. G.; Jones, D.; West, C. E.; Frank, R. A. *Environ. Sci. Technol.* **2011**, *45*, 3154–3159.
- (20) West, C. E.; Scarlett, A. G.; Pureveen, J.; Tegelaar, E. W.; Rowland, J. R. *Rapid Commun. Mass Spectrom.* **2013**, *27*, 357–365.
- (21) Woudneh, M. B.; Coreen Hamilton, M.; Benskin, J. P.; Wang, G.; McEachern, P.; Cosgrove, J. R. *J. Chromatogr. A* **2013**, *1293*, 36–43.
- (22) Headley, J. V.; Peru, K. M.; Barrow, M. P. *Mass Spectrom. Rev.* **2009**, *28*, 121–134.
- (23) Duncan, K. D.; McCauley, E. P. B.; Krogh, E. T.; Gill, C. G. *Rapid Commun. Mass Spectrom.* **2011**, *25*, 1141–1151.
- (24) Lobodin, V. V.; Rodgers, R. P.; Marshall, A. G. In *Comprehensive Environmental Mass Spectrometry*; Lebedev, A. T., Ed.; ILM Publications: St. Albans, U. K., 2012; pp 415–439.
- (25) Marshall, A. G.; Hendrickson, C. L.; Jackson, G. S. *Mass Spectrom. Rev.* **1998**, *17*, 1–35.
- (26) Mapolelo, M. M.; Rodgers, R. P.; Blakney, G. T.; Yen, A. T.; Asomaning, S.; Marshall, A. G. *Int. J. Mass Spectrom.* **2011**, *300*, 149–157.
- (27) Hsu, C. S.; Dechert, G. J.; Robbins, W. K.; Fukuda, E. K. *Energy Fuels* **2000**, *14* (1), 217–233.
- (28) Barrow, M. P.; Witt, M.; Headley, J. V.; Peru, K. M. *Anal. Chem.* **2010**, *82* (9), 3727–3735.
- (29) Nyakas, A.; Han, J.; Peru, K. M.; Headley, J. V.; Brochers, C. H. *Environ. Sci. Technol.* **2013**, *47* (9), 4471–4479.
- (30) Ahad, J. M. E.; Pakdel, H.; Savard, M. M.; Calderhead, A. I.; Gammon, P. R.; Rivera, A.; Peru, K. M.; Headley, J. V. *Environ. Sci. Technol.* **2013**, *47*, 5023–5030.
- (31) Ahad, J. M. E.; Pakdel, H.; Savard, M. M.; Simard, M. C.; Smirnoff, A. *Anal. Chem.* **2012**, *84* (23), 10419–10425.
- (32) Taguchi, V. Y.; Nieckarz, R. J.; Clement, R. E.; Krolik, S.; Williams, R. *J. Am. Soc. Mass Spectrom.* **2010**, *21*, 1918–1921.
- (33) Jobst, K. J.; Shen, L.; Reiner, E. J.; Taguchi, Y. Y.; Helm, P. A.; McCrindle, R.; Backus, S. M. *Anal. Bioanal. Chem.* **2013**, *405*, 3289–3297.
- (34) Kendrick, E. *Anal. Chem.* **1963**, *35*, 2146–2154.
- (35) Sleno, L. J. *Mass Spectrom.* **2012**, *47*, 226–236.
- (36) Hughey, C. A.; Hendrickson, C. L.; Rodgers, R. P.; Marshall, A. G. *Anal. Chem.* **2001**, *73*, 4676–4681.
- (37) Savory, J. J.; Kaiser, N. K.; McKenna, A. M.; Xian, F.; Blakney, G. T.; Rodgers, R. P.; Hendrickson, C. L.; Marshall, A. G. *Anal. Chem.* **2011**, *83* (5), 1732–1736.
- (38) Hunter, E. P.; Lias, S. G. *Proton Affinity Evaluation*, NIST Chemistry WebBook, NIST Standard Reference Database Number 69; Lindstrom, P. J., Mallard, W. G., Eds.; National Institute of Standards and Technology: Gaithersburg, MD, 1999. <http://webbook.nist.gov> (accessed March 17, 2014).
- (39) Harrison, A. G. *Chemical Ionization Mass Spectrometry*; CRC Press Inc.: Boca Raton, FL, 2000; pp 110–114.